Biochimica et Biophysica Acta 1847 (2015) 698–708

Contents lists available at ScienceDirect

Biochimica et Biophysica Acta

journal homepage: www.elsevier.com/locate/bbabio

Effect of lipid bilayer properties on the photocycle of green proteorhodopsin

Ljubica Lindholm, Candan Ariöz, Michael Jawurek, Jobst Liebau, Lena Mäler, Åke Wieslander, Christoph von Ballmoos *[,1], Andreas Barth *

Department of Biochemistry and Biophysics, Stockholm University, SE-106 91 Stockholm, Sweden

ARTICLE INFO

Article history:
Received 4 March 2015
Received in revised form 17 April 2015
Accepted 21 April 2015
Available online 25 April 2015

Keywords:
Proteorhodopsin
Bicelle
Lipid
Detergent
Membrane protein
Photocycle

ABSTRACT

The significance of specific lipids for proton pumping by the bacterial rhodopsin proteorhodopsin (pR) was studied. To this end, it was examined whether pR preferentially binds certain lipids and whether molecular properties of the lipid environment affect the photocycle. pR's photocycle was followed by microsecond flash-photolysis in the visible spectral range. It was fastest in phosphatidylcholine liposomes (soy bean lipid), intermediate in 3-[(3-cholamidopropyl) dimethylammonio] propanesulfonate (CHAPS): 1,2-dioleoyl-*sn*-glycero-3-phosphocholine (DOPC) bicelles and in Triton X-100, and slowest when pR was solubilized in CHAPS. In bicelles with different lipid compositions, the nature of the head groups, the unsaturation level and the fatty acid chain length had small effects on the photocycle. The specific affinity of pR for lipids of the expression host *Escherichia coli* was investigated by an optimized method of lipid isolation from purified membrane protein using two different concentrations of the detergent *N*-dodecyl-β-D-maltoside (DDM). We found that 11 lipids were copurified per pR molecule at 0.1% DDM, whereas essentially all lipids were stripped off from pR by 1% DDM. The relative amounts of copurified phosphatidylethanolamine, phosphatidylglycerol, and cardiolipin did not correlate with the molar percentages normally present in *E. coli* cells. The results indicate a predominance of phosphatidylethanolamine species in the lipid annulus around recombinant pR that are less polar than the dominant species in the cell membrane of the expression host *E. coli*.

1. Introduction

Proteorhodopsin (pR) is a natural photoactive protein embedded in the lipid bilayer of many bacteria found in the sea and salt lakes. First discovered in the gammaproteobacteria 'SAR86' group [1], it was subsequently also found in alphaproteobacteria [2], archaea [3], bacteroidetes [4], eukaryotes [5] and viruses which are thought to have acquired the pR gene from bacteria [6].

Like the archaeal bacteriorhodopsin (bR), pR contains the retinal chromophore bound via a Schiff base linkage to a lysine residue in the seventh transmembrane segment (Lys231 in pR) and adopts several intermediates after light excitation. The photocycle of pR is shown in Fig. 1. It is similar to that of bR in which light excitation of the retinal induces conformational changes in the protein, resulting in the translocation of a proton across the membrane. Since the chromophore retinal exhibits a high spectral sensitivity towards its environment, the photocycle can be monitored by the transient absorbance changes at different wavelengths [7]. In the first step of the photocycle, the retinal isomerizes from all-*trans* to 13-*cis* upon transition from the pR ground state (named pR 520 in Fig. 1) to the K intermediate. This is followed by deprotonation of the Schiff base and protonation of the primary proton acceptor Asp-97 upon formation of the M state ($\lambda = 410$ nm), which may consist of two substates M_1 and M_2 [8]. The decay of the M-intermediate reflects reprotonation of the Schiff base and gives rise to the formation of late intermediates. The first of them is observed near $\lambda = 560$–580 nm and is termed O [7] or N [8]. The following intermediate absorbs near the pR absorption maximum and is termed N by Friedrich et al. [7] who observe it near 530 nm, but is named pR′(O) by Varo et al. [8] who consider its absorption as indistinguishable from that of pR. Eventually, the retinal isomerizes back to the all-*trans* configuration by thermal relaxation and the proton gradient created by pR is used for ATP synthesis. In Fig. 1 and in the following, we name the intermediates according to Friedrich et al. [7].

Abbreviations: bR, bacteriorhodopsin; CHAPS, 3-[(3-cholamidopropyl)dimethylammonio] propanesulfonate; CL, cardiolipin; DDM, *N*-dodecyl-β-D-maltoside; DMPC, 1,2-dimyristoyl-*sn*-glycero-3-phosphocholine; DMoPC, 1,2 dimyristoleoyl-*sn*-glycero-3-phosphocholine; DOPA, 1,2-dioleoyl-*sn*-glycero-3-phosphate; DOPC, 1,2-dioleoyl-*sn*-glycero-3-phosphocholine; DOPE, 1,2-dioleoyl-*sn*-glycero-3-phosphoethanolamine; PC, phosphatidylcholine; PE, phosphatidylethanolamine; PG, phosphatidylglycerol; POPE, 1-palmitoyl-2-oleoyl-*sn*-glycero-3-phosphoethanolamine; pR, proteorhodopsin; TOCL, tetraoleoyl cardiolipin; TLC, thin layer chromatography.

* Corresponding authors at: Department of Biochemistry and Biophysics, Arrhenius Laboratories, Stockholm University, SE-106 91 Stockholm, Sweden.
E-mail addresses: christoph.vonballmoos@dcb.unibe.se (C. von Ballmoos), barth@dbb.su.se (A. Barth).
[1] Present address: Department of Chemistry and Biochemistry, University of Berne, Freiestrasse 3, CH-3012 Bern, Switzerland.

http://dx.doi.org/10.1016/j.bbabio.2015.04.011
0005-2728/

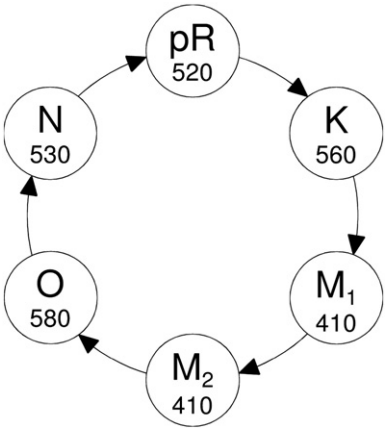

Fig. 1. Simplified photocycle of pR according to [8] in the terminology of [7]. Numbers denote the absorbance maximum of the respective state. The photocycle starts with excitation of the ground state of pR which is named pR 520 in the above scheme.

The native lipid environment of green absorbing proteorhodopsin (Uniprot accession code: Q9F7P4) is not precisely known as pR studied so far has been recombinantly overexpressed in *Escherichia coli* (*E. coli*). The *E. coli* membrane is a valid starting point for testing the lipid effect on pR's photocycle because the marine bacteria, in which pR was originally discovered, have a similar phospholipid composition as *E. coli* [2,9–14]. The head group composition of phospholipids in *E. coli* remains constant over a broad spectrum of growth conditions [15]. The aminophospholipid phosphatidylethanolamine (PE) is the major phospholipid in *E. coli* constituting 70–80% of the total phospholipid content. It is zwitter-ionic at physiological pH due to the protonated amino group and the negatively charged phosphate group. PE is accompanied in the membrane by the two anionic lipids, phosphatidylglycerol (PG) and cardiolipin (CL), accounting for 15–20% and ≤5% of the membrane phospholipids, respectively [16].

In order to understand more about the conditions affecting pR's photocycle, detailed knowledge about the interactions of wild type green pR with membrane lipids is important. It is well known that lipids can affect the activity of membrane proteins through stable or dynamic interactions. As an example, charged protein residues can readily interact with lipids through electrostatic interactions and form hydrogen bonds (H-bonds) with lipid head groups [17]. It has been observed that the hydrophobic thickness of the lipid bilayer is an important factor for the correct topology and insertion of a membrane protein and consequently for its optimal function [18,19]. Many membrane proteins are known to prefer specific lipids, for example the Ca^{2+} ATPase prefers phosphatidylcholine (PC) over PE for optimum activity [20], the respiratory complexes II–IV are CL dependent [21], and KcsA requires anionic lipids for optimum activity [22]. The activity of bR, is reported to be influenced by several lipids [23,24], and a brief treatment of the purple membrane with low concentrated detergent causes changes of the bR photocycle without disrupting the trimer structure of bR [24] indicating a strong dependence of bR activity on native membrane lipids. This assertion is verified by the recovery of normal photocycle behavior by incubating the disrupted membranes with a total extract of the native lipids from the purple membrane [24].

pR has earlier been studied in different lipid and detergent environments [7,25]. However, no systematic investigation has been done regarding the effects of lipids on the photocycle. Therefore, the aim of our research was to identify and understand how the lipophilic and amphiphilic environment shapes pR activity. In this study, we have mainly used bicelles, which are also known as mixed micelles, consisting of a mixture between CHAPS and a phospholipid. Specifically, we tested the influences of different types of lipid head groups, various fatty acid chain-lengths and the extent of saturation in the fatty acid chain on the pR photocycle. Furthermore, we analyzed lipids that are copurified with pR using two different detergent concentrations in order to detect whether pR specifically binds certain lipids. Taken together, we observed that an intact membrane is beneficial for optimum function but that particular lipid properties have only small effects.

2. Materials and methods

2.1. Chemicals and buffers

Most lipids used in our experiments were purchased from Avanti Polar Lipids (Alabaster, AL). Soy bean type II-S lipids and CHAPS were purchased from Sigma Aldrich and *N*-dodecyl-β-D-maltoside (DDM) from Affymetrix. Other chemicals were all obtained from Sigma Aldrich.

2.2. Cloning, growth, purification and reconstitution of unlabelled pR

The wild type green pR gene was synthesized by Eurofins MWG Operon (Ebersberg, Germany) and cloned into a pET27b+ (Invitrogen) vector using NdeI and XhoI as cloning sites [7]. A C-terminal His_6-tag was included in this construct to facilitate pR purification with Ni-NTA affinity purification. C43 (DE3) [26] was used as an expression host for pR. pR was expressed and purified as described by Pfleger et al. [27] with the exception that DDM was exchanged for CHAPS during the Ni-NTA purification step for pR intended for bicelle studies.

Proteoliposomes from soy bean phosphatidylcholine were prepared by a freeze–thaw procedure. In brief, 30 mg lipids dissolved in chloroform were dried in a round bottomed flask by a stream of nitrogen and 2 h of vacuum. The lipids were then resuspended in 3 ml reconstitution buffer (50 mM MOPS, pH 7.5, 50 mM NaCl) and vortexed for 10 min at room temperature under nitrogen atmosphere. Liposomes were made unilamellar and homogeneous in size by a tip sonicator on ice (Sonics, VCX130PB, 6 cycles, 30 s pulse, 30 s pause, 40% output). For reconstitution, 100 μl of 1 mg/ml pR was added to 1 ml of liposome suspension and frozen in liquid nitrogen and thawed in water. The freeze–thaw cycle was repeated once. For flash photolysis measurements, 100 μl of liposomes was diluted with 400 μl reconstitution buffer.

We checked our reconstitution of pR into liposomes using a pH sensitive dye on the inside of the liposomes. The light induced proton pumping experiments indicate that pR is functionally incorporated and that the majority of pR molecules are oriented such that they pump protons to the inside of the liposomes.

2.3. Overexpression and purification of pR for the analysis of tightly bound lipids

In order to analyze lipids that bind to pR with high affinity, phospholipids were radioactively labeled during pR expression by supplying the growth medium with [1-^{14}C] sodium acetate (Perkin-Elmer). Two ml of overnight culture was used to inoculate 200 ml of 2× Luria Bertani (LB) medium supplemented with 50 μg/ml kanamycin and 1 μCi/ml ^{14}C acetate (Large culture). The culture was grown at 37 °C at 200 rpm. When OD_{600} reached 0.8, isopropyl-β-D-1-thiogalactopyranoside (IPTG) and all-*trans* retinal (Sigma-Aldrich) in ethanol were added to final concentrations of 1 mM and 0.44 mM, respectively. The cells were kept at 37 °C, 200 rpm for 4 h and harvested by centrifugation (3000 ×*g*) for 20 min at 4 °C. The cells were suspended in 50 mM MES buffer pH 6.0, containing 300 mM NaCl, and disrupted mechanically with a glass homogenizer. The cell lysate was centrifuged for 1 h at 3700 ×*g* in a top bench centrifuge at 4 °C and the membrane pellet was further solubilized for 48 h in 50 ml of 50 mM MES pH 6.0 buffer, containing 300 mM NaCl, 5 mM imidazole and either 1% or 0.1% DDM.

Detergent solubilized protein was obtained by centrifugation at 150,000 ×*g* for 45 min at 4 °C and the supernatant was incubated with 4 ml of Ni-NTA beads overnight at 4 °C. After binding of pR to the resin, the resin beads were washed with wash buffer containing 0.1% Triton and 50 mM imidazole, followed by a second wash with 900 ml

deionized water to remove impurities and excess detergent molecules since DDM interferes with the lipid analysis of endogenous lipids copurified with pR. The pR bound to the Ni-NTA resin was kept frozen at −20 °C overnight and the lipid analysis was performed as described in Section 2.5.

2.4. Preparation of whole E. coli lipid extracts

For the lipid analysis of total *E. coli* membrane lipids of induced and uninduced cells, two cell cultures of 10 ml 2× LB supplemented with 0.2 μCi/ml of [1-^{14}C] acetate (Perkin Elmer, 55.3 mCi/mmol) were grown in parallel with the large culture. 0.44 mM all-*trans* retinal (Sigma Aldrich) was added to the uninduced samples when OD_{600} = 0.8 while both 0.44 mM all-*trans* retinal (Sigma Aldrich) and 1 mM IPTG were added to the induced samples. The cell cultures were grown further for 4 h of induction and then harvested at 3000 ×*g* for 20 min at 4 °C. The cell pellets were stored at −20 °C overnight and the lipids were extracted from the cell pellets using the Bligh & Dyer extraction protocol [28]. The extracted lipids were dried completely under N_2 gas and then redissolved in 200 μl methanol/chloroform 2/1 (v/v).

2.5. Analysis of endogenous lipids copurified with pR

The Ni-NTA resins containing the purified pR (see Section 2.3) were mixed with 30 ml methanol and transferred to a clean (lipid free) glass separatory funnel. Afterwards, 60 ml chloroform was added to yield a chloroform/methanol ratio of 2/1. For lipid analysis with thin layer chromatography (TLC), special care had to be taken to remove all remainders of detergent because DDM as an amphiphilic molecule migrates to the chloroform/methanol phase during lipid extraction and interferes with the subsequent step of TLC lipid analysis. In order to remove the excess detergent, the chloroform/methanol phase was washed extensively with 4 l of double distilled water and the chloroform phases were recovered again. This washing step might carry away a small percentage of lipids into the aqueous phase but was necessary to get a clear separation of the lipids on the TLC plates. It was tried to omit the washing step but this gave unsatisfying resolution under all conditions tested.

The lipid extracts (chloroform phases) were dried completely under N_2, yielding a thin lipid film. This film was redissolved in 1 ml chloroform/methanol (ratio 2/1) and 500 μl from this preparation was applied on standard Silica gel 60 TLC plates (Merck) in parallel with 50 μl total cell lipid extracts obtained from 10 ml cultures of induced and uninduced cells (as described in Section 2.4). This was repeated for two different plates (0.1% and 1% DDM solubilization).

The TLC plates were developed in single dimension using chloroform/methanol/acetic acid 85/25/10 (v/v/v) as the mobile phase. The lipid spots were visualized and quantified by electronic radiography using Image Gauge version 4.0. The radioactivity of each lipid spot was calculated using a calibration curve obtained from the responses of a concentration series of eight [1-^{14}C] acetic acid samples, which were placed on the dried, developed TLC plate before the exposure, ranging from 25 to 2500 nCi. The responses were completely linear for the series, with $R^2 \geq 0.99$.

In order to estimate the number of bound lipids per pR, the total numbers of lipids in the total lipid extracts were calculated in two steps: (i) the number of cells was estimated from the absorbance at 600 nm (OD_{600}) [29]. (ii) The total number of phospholipids for this number of cells was calculated from the number of lipids per cell (http://ccdb.wishartlab.com/CCDB/cgi-bin/STAT_NEW.cgi). Then, the radioactivity of the spots from the copurified lipids was related to that from the total lipid extract, giving the total number of phospholipids attached to pR after solubilization in 0.1% and 1% DDM. Finally this number was related to the amount of protein produced in the 200 ml cultures (Section 2.3) as determined from measuring the protein concentration of a small portion of the obtained protein sample.

2.6. Preparation of bicelles

Bicelles were prepared according to a published protocol [30]. Briefly, 8 mM of the desired lipid composition was solubilized in chloroform/methanol (2/1, v/v), and then the solvent was evaporated under a stream of gaseous nitrogen. The remaining organic solvent was removed in a Speed Vac. Lipid mixtures were then solubilized to homogeneity in 50 mM MOPS, pH 7.8, 50 mM NaCl, 16 mM CHAPS buffer by extensive vortexing, followed by water bath sonication for 5 min. The q-value (molar lipid to detergent ratio) of the bicelles was 0.5. The bicelle samples for solution NMR were produced in the same way with the only difference that D_2O buffer (50 mM MOPS, pD 7.8, 50 mM NaCl, 16 mM CHAPS) was used to hydrate the dried lipid film.

2.7. Laser flash photolysis spectroscopy

Time dependent absorption spectroscopy after flash photolysis was used to investigate the photocycle of pR. Spectroscopic measurements were performed at room temperature (22–23 °C) using a custom built flash photolysis setup [31]. Briefly, light at the desired wavelength (410, 500, 580 and 630 nm) was obtained from a white light source and passed through a monochromator (Applied Photophysics) and directed to a cuvette containing the pR sample. Absorption changes were detected with a photomultiplier tube (PMT) and recorded by an oscilloscope with a time resolution of 1 μs. pR was excited with a laser pulse (10 ns, 200 mJ, 532 nm, Nd:YAG Brilliant B, Quantel) which was oriented 90° to the measuring light beam. To prohibit PMT saturation by the laser pulse, a bandpass filter (5 nm) of the desired wavelength was mounted in front of the PMT.

Experiments were performed with pR solubilized in the detergents CHAPS and Triton X-100 as well as in CHAPS containing bicelles and in liposomes. Typically, 20 traces were recorded (with intervals of >5 s) and averaged. To minimize artifacts from local bleaching, the cuvette was taken out and shaken after 5 measurements. The traces of these 5 measurements were indistinguishable. A fresh sample of pR was used for measurements at each wavelength. The initial absorbance change at 500 nm after the laser pulse reflects the amount of reactive pR in our samples. Therefore, it was used to normalize the signals obtained at this wavelength but also the signals of the corresponding samples measured at the other three wavelengths. The kinetic data were analyzed by simultaneous (global) fitting of a single kinetic model to the four transient absorbance changes at 410, 500, 580 and 630 nm using the KinTek Global Explorer software (KinTek Corp. Austin Texas) [32,33]. The kinetic model was a series of irreversible reactions and was simulated by a sum of five exponential functions with time constants T_1 to T_5. The accuracy of the time constants (indicated as ±) was calculated by the 1D FitSpace algorithm (within KinTek Global Explorer), which tests the range of each time constant within the applied global fit, while all other parameters are allowed to float freely [33].

2.8. Translational diffusion NMR experiments

Diffusion experiments were recorded using a Bruker Avance spectrometer operating at 9.4 T (400 MHz ^{1}H frequency). ^{1}H diffusion experiments for bicelles containing either PC 18:1 or PC 20:1 lipids and CHAPS (q = 0.5) were carried out at 22 °C. Translational diffusion coefficients were determined using a modified Stejskal–Tanner spin-echo pulse sequence with a fixed diffusion time and a pulsed field gradient increasing linearly over 32 steps [34–36]. The gradient was calibrated on the ^{1}H signal of a standard sample containing 1% H_2O in D_2O, 1 mg/ml $GdCl_3$ and 0.1% DSS. The translational diffusion coefficients of the bicelles were determined using the ^{1}H signal of the g2 proton in the PC lipid at 5.20 ppm [37] by fitting the attenuation of the signal at

increasing pulsed field gradient strengths to the Stejskal–Tanner equation. Viscosity differences were accounted for by measuring the translational diffusion coefficient of HDO in the bicelle sample and comparing it to its diffusion in H_2O [38]. The obtained factor was used to normalize, i.e. viscosity-correct, the bicelle diffusion coefficient. The hydrodynamic radius was calculated with the Stokes–Einstein equation including a shape factor of 1.2 that accounted for the non-spherical shape of bicelles [39]. Experimental errors were estimated by repeating all diffusion experiments 5 times. The obtained diffusion coefficients for the PC lipids reflect the translational diffusion of the bicelles since the solubility of 18:1 and 20:1 PC in water is negligible. Moreover, the tumbling of the bicelles is fast compared to the diffusion delay (typically 0.4 s) averaging lateral diffusion of lipids in the bilayer to zero [40].

3. Results

3.1. Membrane lipids in pR's native hosts

In order to identify relevant lipids that might affect the activity of pR, we reviewed available lipid data and analyzed the genome of organisms containing the pR gene. Three approaches were applied: (i) for well-established pR genes from uncultivated organisms or ones lacking complete genome information, the lipid composition in closely related phylogenetic organisms was checked [2,9]. (ii) From organisms without lipid data but with completely sequenced genomes containing a pR gene, genes for key phospholipid enzymes were searched by BLAST using the corresponding amino acid sequences from *E. coli* as probes (genomes from *Dokdonia* sp. MED134 [11] and gamma proteobacterium HTCC2207). (iii) In addition, the experimentally determined lipid compositions from several proteobacteria (having a pR gene) [10,13,14,41] were also considered.

The three major *E. coli* phospholipids PE, PG, and CL were either predicted or are the dominating lipids found experimentally. However, for the organisms for which experimental data are available, the proportions between PE, PG and CL vary. In addition, some other, minor species have also been observed. Hence, given this coherent composition and the functional expression of pR in *E. coli*, the PE, PG and CL lipids seem to be physiologically relevant candidates for the analysis of pR's lipid dependence.

3.2. Analysis of lipids that tightly bind to pR overexpressed in E. coli

Given the above analysis of the lipid composition of organisms containing the pR gene, *E. coli* seems to be a suitable host for the expression of pR. Accordingly, we wanted to test whether a specific *E. coli* lipid, which might be essential for the pR's activity, is retained by pR after its solubilization. In order to detect tightly bound lipids after protein purification, we labeled membrane lipids by supplementing the growth media with radioactive acetate, a precursor for lipid synthesis. After harvesting the cells, pR was solubilized and isolated via affinity chromatography, and the co-purified lipids were extracted with organic solvents and analyzed by autoradiography of TLC plates. Extensive washing of the organic phase after lipid extraction with water ensured complete removal of excessive detergent molecules, as indicated by sharp straight bands in the TLC experiments. Two different detergent concentrations (0.1% and 1% DDM) were used in order to determine the affinity of pR to lipids in the *E. coli* membrane. In the experiments with 1% DDM, only ~0.1 lipid per pR monomer was found, indicating that essentially all lipids were stripped off. With 0.1% DDM however, ~11 lipids were copurified per pR monomer (Table 1), revealing binding of lipids under these conditions.

The total *E. coli* lipid extract contained approximately 75 mol% PE (zwitter-ionic), 25 mol% PG (anionic) and less than 5 mol% CL (dianionic), as can be seen in Fig. 2 (lanes 1 and 2) which correlated well with previous studies [42]. In contrast, the lipids bound to pR after 0.1% DDM treatment were 92 mol% PE, 6 mol% PG and 2 mol% CL (Fig. 2 and Table 1) indicating that PE dominates the annular lipids around pR. However, the fraction of bound PE decreased from 92% to 61% when 1% DDM was used for solubilization and the percentage of bound CL increased (Table 1). Since DDM and PE can both interact with the protein surface via hydrogen bonding, the reduced PE binding at the higher DDM concentration could be due to competition between DDM and PE molecules. The relatively increased amount of bound CL at the higher DDM concentration might be explained by its stronger hydrophobicity compared to PE, which could make it more difficult to exchange.

It is interesting to note that the copurified PE and to a minor extent the copurified PG migrate further than the bulk lipids. We therefore performed controls to assure that the assignment to PE and PG is correct. The first test indicated that the different migration behaviors are not due to an "unusual" head group. Lipids with alternative head groups, like phosphatidylserine and phosphatidic acid, migrated very differently from PE, PG and CL. In addition, a ninhydrin test confirmed that the major copurified lipid contains an amine group and that it therefore has a PE head group. This is an indication that pR selects a subpopulation of the PG and PE lipids, which has more hydrophobic acyl chains. These lipids might have longer acyl chains, a higher degree of saturation, less cyclopropanation or methylated acyl chains. A further point of interest is the increased CL content of the induced cells which is most clearly seen in Fig. 2B (compare lanes 1 and 2). This effect is often observed upon overexpression of membrane proteins, for example in our previous work on MGS [43].

In addition to the TLC bands discussed above, there are up to four further bands nearer to the migration front. The hydrophobic molecules that give rise to these bands seem not to be bound to pR because they have been observed also in a control experiment in which *E. coli* cells were transformed with a plasmid not containing pR and subjected to our protein purification protocol, followed by lipid extraction and TLC

Table 1
Estimated bound phospholipids per detergent purified pR monomer.

Number of bound lipids	0.1% DDM	1% DDM
PE	10.4 (92%)	0.11 (61%)
PG	0.64 (6%)	0.02 (11%)
CL	0.22 (2%)	0.05 (28%)

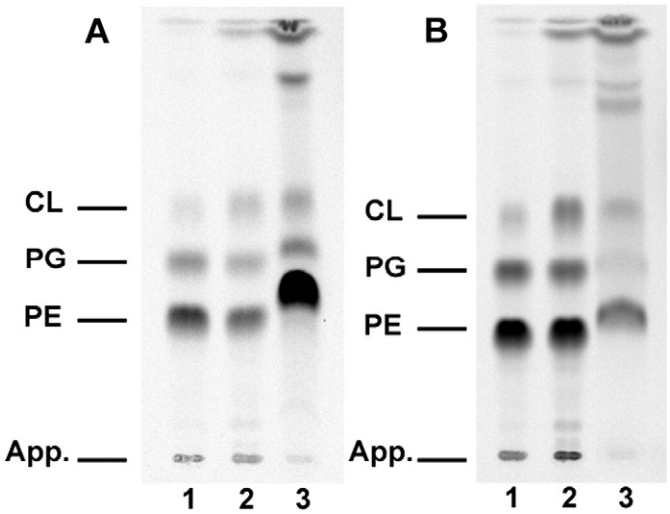

Fig. 2. TLC analysis of lipids that copurify with pR in the presence of 0.1% DDM (plate A) and 1% DDM (plate B). The acyl chains of the lipids were radioactively labeled with ^{14}C-acetate during pR overexpression. Lanes 1 and 2 show the polar lipids extracted from uninduced and IPTG-induced cultures, respectively, and lane 3 shows the copurified lipids bound to the purified pR.

analysis. The TLC plates showed the bands above CL but not the phospholipid bands seen in Fig. 2 (lane 3 in panels A and B).

3.3. Bicelle model system

In order to test the influence of a phospholipid environment on the photocycle of pR, bicelles with a defined detergent to lipid ratio were used. Such systems have proven to be useful for a variety of applications. They are bilayer like organizations [30,44] and have the advantage over liposomes of reduced light scattering and therefore enable a better signal to noise ratio in the optical flash photolysis experiments. In the bicelles, the ratio between the detergent CHAPS (16 mM) and other lipids (8 mM) was kept constant but the types of lipids differed for different preparations. CHAPS, a non-ionic detergent, was chosen for this study because it is known to form bicelles in the presence of phospholipids.

A main advantage of bicelles for our study was the reduced light scattering as compared to turbid liposomes samples in spectroscopic measurements. Furthermore, the convenient preparation of pR–bicelle complexes by mixing purified pR solubilized in CHAPS and preformed lipid preparations ensured controlled and reproducible conditions. In the following, different lipid properties were tested for their effect on the photocycle comprising head group charge, fatty acid chain length and degree of unsaturation. For most lipids tested, we chose fatty-acyl chains with one *cis* double bond as these occur naturally in *E. coli*. In addition, this ensured that the lipids were in the fluid phase when the experiments were carried out at room temperature.

3.4. PC 18:1 and 20:1 form bicelles together with CHAPS

To characterize the CHAPS/lipid mixtures, we used pulsed field gradient diffusion NMR. The translational diffusion coefficient is linked to the hydrodynamic radius of the aggregate via the Stokes–Einstein equation. The diffusion coefficients and hydrodynamic radii for mixtures containing either 18:1 PC (DOPC) or 20:1 PC (1,2-dieicosenoyl-*sn*-glycero-3-phosphocholine) lipids are given in Table 2. The hydrodynamic radii of both types of mixtures are typical for small, isotropic bicelles made with CHAPS [44], smaller than bicelles with DHPC ($q = 0.5$), but significantly larger than CHAPS micelles at the concentration used here (20 mM) [45,46]. Moreover, we see that 18:1 PC/CHAPS bicelles are somewhat smaller than 20:1 PC/CHAPS bicelles. We conclude that both lipids are incorporated into CHAPS containing bicelles, and form structures that are larger than CHAPS micelles.

To assure that the incorporation of pR into the bicelles did not alter the morphology of the CHAPS/lipid mixtures, diffusion experiments were carried out also on bicelles with added protein. Table 2 reports the diffusion coefficients and hydrodynamic radii for bicelles with and without pR. The hydrodynamic radius was in all cases around 3 nm. The addition of pR leads only to minor changes in the hydrodynamic radii of the bicelles, as expected since the protein concentration is around an order of magnitude lower than that of bicelle assemblies. The most likely explanation for the observed slight decreases in the hydrodynamic radii is that there are two populations of bicelles, the majority being bicelles with a higher content of detergent, which makes them smaller, together with a few larger ones containing pR. This would overall lead to a slight reduction in average size. Most importantly, the differences are small and we conclude that the addition of protein does not lead to a major change in bicelle morphology.

Table 2
Normalized translational diffusion coefficients D_t[a] and hydrodynamic radii r_H for 18:1 PC and 20:1 PC in bicelles with and without incorporation of pR.

	18:1 PC[b]	18:1 PC[b] + pR	20:1 PC[c]	20:1 PC[c] + pR
D_t [10^{-11} m^2 s^{-1}]	7.2 ± 0.1	7.8 ± 0.1	6.4 ± 0.1	7.2 ± 0.2
r_H [nm]	2.8	2.6	3.2	2.8

[a] Determined using the g2 ^{1}H signal in PC at 5.20 ppm and viscosity-corrected based on the diffusion of HDO in the sample.
[b] DOPC.
[c] 1,2-dieicosenoyl-*sn*-glycero-3-phosphocholine.

3.5. Contribution of photocycle intermediates to the transient absorbance changes

pR's photocycle was studied by flash photolysis with purified pR reconstituted in detergents, bicelles, and liposomes. This technique has been proven to be very useful to reliably monitor the photocycle of bR and pR. After the sample had been excited by a short laser pulse at 532 nm (close to the maximal absorption at 520 nm), transient absorbance changes were measured at 410, 500, 580, and 630 nm. Spectra of the photocycle intermediates have been published [8] and can be used to estimate the contribution of each intermediate to the absorption at the four wavelengths used. In our discussion we will adopt the terminology of Friedrich et al. [7].

At 410 nm, the M intermediate absorbs 3–4 times stronger than the other intermediates and the pR ground state. Therefore, this wavelength reflects predominantly the formation and decay of the M intermediate. At all other wavelengths used in this study, the absorption of the M intermediate is negligible.

At 500 nm, the pR ground state and the last intermediate N absorb equally and about twice as strong as the other intermediates. Thus, the signal at this wavelength will be dominated by the time-dependent concentrations of the ground state and of the N intermediate.

At 630 nm, O and K intermediates absorb strongest, whereas the pR groundstate and the N intermediate have negligible absorbance. Thus the signal will be dominated by the concentration of K in the early phase of the photocycle and by that of O in the late phase. The situation is similar at 580 nm, but pR and N also contribute to the signal since their absorbance is 1/3 of that of the O intermediate.

3.6. The photocycle in detergents, bicelles and liposomes

In the first set of experiments, we tested the influence of different membrane mimetic environments on the general turnover of pR, as estimated from reformation of the ground state (observed at 500 nm) (Fig. 3A). Due to light scattering, the trace of the transient absorbance change obtained with liposomes shows larger noise.

The transient absorbance change at 500 nm is dominated by the concentrations of the ground state and the N intermediate (see Section 3.5) and reflects therefore the overall turnover of the photocycle. It exhibits a sudden drop in absorbance immediately after the excitation flash due to depletion of the ground state. This initiation of the photocycle cannot be resolved kinetically with our method. Subsequently, the absorbance increases back to its initial value because the N intermediate is formed and the ground state is restored. Since the N intermediate and the ground state have similar absorption spectra (see Introduction and Section 3.5), the absorbance increase is probably dominated by the formation of the N intermediate. The subsequent decay of N and the reformation of the pR ground state are expected to have a smaller influence on the signal.

The absorbance increase due to N formation and restoration of the ground state can be fitted to a two-step reaction, if no reverse reaction is allowed. The faster reaction contributed to >80%. The reaction model was fitted to the data at individual wavelengths in this section. Therefore the time constants in this section should not be compared with the time constants obtained by global fitting to all 4 wavelengths simultaneously, which are listed in Tables 3 and 4.

As depicted in Fig. 3A, formation of the late N intermediate and restoration of the ground state are fastest for pR reconstituted in soy bean liposomes (time constants ~12 and ~100 ms) followed by CHAPS/DOPC bicelles (~20 and ~140 ms), Triton X-100 (~40 and ~500 ms) and slowest in CHAPS (~80 and 1000 ms). Accordingly, turnover turned

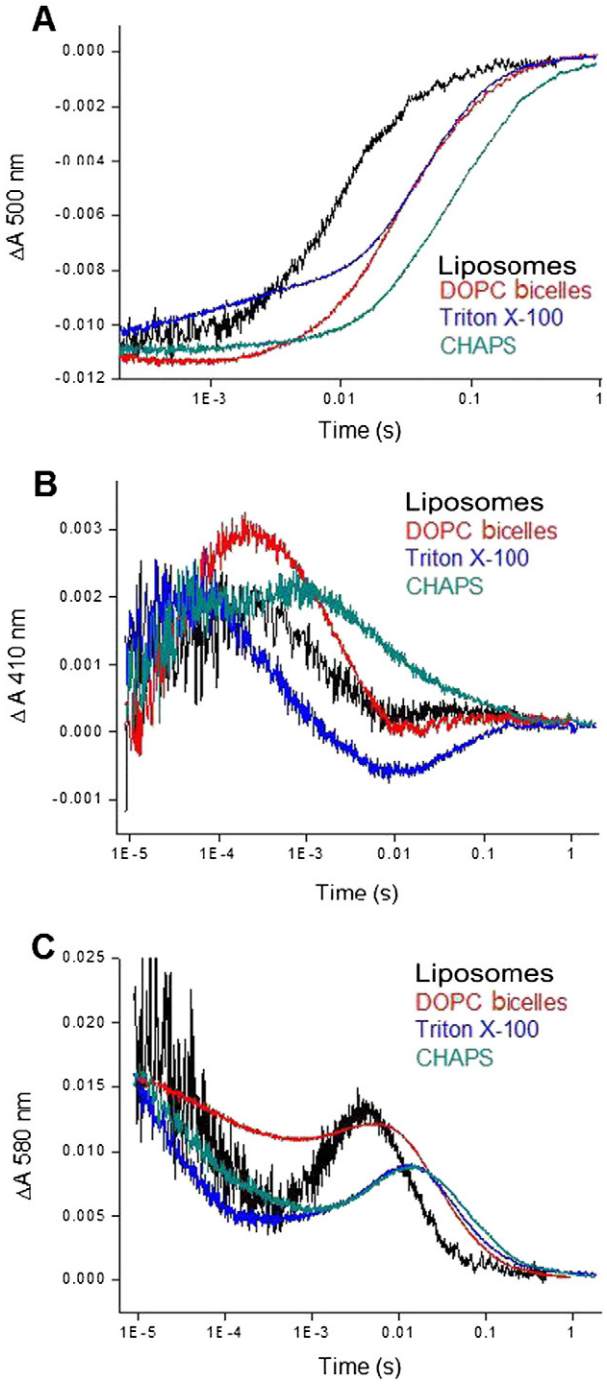

Fig. 3. Time-resolved spectroscopy of detergent (Triton X-100 and CHAPS) solubilized pR, pR in bicelles with the zwitter-ionic lipid DOPC and pR in soy bean liposomes at three different wavelengths: (A) 500 nm, (B) 410 nm, and (C) 580 nm.

out to be fastest in the "native" environment of a liposome. DOPC liposomes have also been tested and gave similar results to soy bean lipids (data not shown).

The slowdown of the turnover rate in CHAPS compared to Triton X-100 is not surprising, as CHAPS is considered a stiff detergent due to the rigid steroid ring structure, possibly impairing the motional flexibility of pR. However, upon mixing the slow CHAPS preparation with lipids in order to form bicelles, turnover was accelerated up to 4-fold, reaching 60% of the activity in soy bean liposomes. Thus the addition of lipids to the CHAPS detergent micelles makes the lipid environment of pR more similar to that in liposomes. Most likely, this is due to a replacement of CHAPS by lipids in the immediate vicinity of pR.

Table 3
Time constants of the pR photocycle in different lipid environments obtained with preparation 1. The time constants T_1 to T_5 were determined as described in the Materials and methods. Two pR preparations in CHAPS were used. The results for preparation 1 are listed in this table and those for preparation 2 in Table 4. Results with the same preparation are directly comparable, whereas slightly different pR/CHAPS/lipid ratios in the two preparations might affect the rates and thus the comparability between the two sets of experiments.

	T_1/μs	T_2/μs	T_3/ms	T_4/ms	T_5/ms
18:1 PG (DOPG)	44 ± 3	680 ± 110	1.7 ± 0.2	19.6 ± 1.8	91 ± 8
16:0–18:1 PE (POPE)	61 ± 10	530 ± 140	2.2 ± 0.2	17.5 ± 1.7	91 ± 8
16:0–18:1 PC (POPC)	39 ± 4	420 ± 50	2.8 ± 0.2	22.7 ± 1.5	108 ± 13
20:1 PC[a]	41 ± 9	790 ± 310	1.9 ± 0.8	18.2 ± 2.3	91 ± 11
18:1 PC (DOPC)	39 ± 4	490 ± 120	3.0 ± 0.2	20 ± 2	91 ± 8
16:1 PC[b]	38 ± 2	680 ± 200	2.0 ± 0.3	19 ± 2	111 ± 11
14:1 PC (DMoPC)	33 ± 2	580 ± 100	2.1 ± 0.1	31 ± 4	167 ± 13
14:0 PC (DMPC)	26 ± 1	480 ± 60	3.2 ± 0.2	37 ± 4	169 ± 16

[a] 1,2-Dieicosenoyl-*sn*-glycero-3-phosphocholine.
[b] 1,2-Dipalmitoleoyl-*sn*-glycero-3-phosphocholine.

Table 4
Time constants of the pR photocycle in different lipid environments obtained with preparation 2. See Table 3 for further information.

	T_1/μs	T_2/μs	T_3/ms	T_4/ms	T_5/ms
DOPC	39 ± 8	410 ± 120	2.9 ± 0.5	21 ± 2	95 ± 11
DOPC/DOPG (9/1)	51 ± 12	440 ± 140	3.5 ± 0.4	26 ± 4	120 ± 18
DOPC/DOPA (9/1)	53 ± 7	590 ± 140	3.5 ± 0.3	26.3 ± 3.5	114 ± 15
DOPC/TOCL (9/1)	47 ± 3	490 ± 100	3.6 ± 0.2	28.7 ± 2.3	135 ± 16

In the following, we compare the kinetics of several photocycle intermediates in the different reconstitution forms. Above pH 7, formation of the M state is observed at 410 nm (Fig. 3B) as an absorbance increase due to deprotonation of the Schiff base. The following absorbance decrease indicates the decay of the M intermediate and is interpreted as the re-protonation of the Schiff base from the P-side, presumably coupled to proton uptake from the medium. The Triton trace shows a very rapid M formation (~8 μs) and an M decay with a time constant of around ~0.5 ms. With CHAPS, M formation is slightly slower (17 μs), the M state persists for a longer time and decays considerably slower (~13 ms) than with Triton. The kinetics of liposomes and bicelles are very similar, with M formation times of ~70–80 μs and M decay times of ~1–2 ms. The slow M decay in the stiff detergent CHAPS indicates that reprotonation of the Schiff base, which takes place during M decay, requires conformational mobility of the protein. This mobility seems to be hampered in CHAPS, but seems to be recovered when CHAPS is supplemented by lipids in our bicelles.

The absorption at 580 nm monitors predominantly the K and the O state with contributions from the N and the ground state (see Section 3.5). The signal (Fig. 3C) rises instantaneously due to the formation of the K intermediate. Its following decay attenuates the absorbance. Formation of the late N and O intermediates leads to a second increase in absorbance and their decay to the final decrease of the signal. Again, traces from pR reconstituted in soy bean liposomes or DOPC bicelles display a faster formation of the late intermediates with time constants of ~2 ms and 3 ms (time constants derived from fits to the 580 nm trace only), respectively, while the two detergent samples display a distinctly later formation of these intermediates (~6–7 ms).

Taken together, we have observed that CHAPS delays the overall photocycle drastically. In contrast, the rates and curve shapes of pR in bicelles are closer to those in liposomes and we can conclude that bicelles are a suitable system for a systematic study on the influence of lipid properties on the photocycle of pR.

3.7. Effect of lipid head groups on the pR photocycle

The influence of lipid head group properties on the photocycle of pR was also studied. Here and in the following sections, the data were analyzed by global fitting, i.e. the data at the four different wavelengths

were fitted simultaneously to a sum of five exponential functions with different time constants. A global fit is a mathematical solution (with a fixed set of parameters) to observed traces and it is difficult to assign the results to specific chemical reactions, as the obtained mathematical solution is often not unique. However, the following approximate assignment can serve as a rough guideline: the smallest time constant T_1 is related to the decay of the early K intermediate and formation of the M intermediate. Time constants T_2 and T_3 are associated with the decay of the M intermediate (see below for further discussion). Mainly time constant T_3 relates to formation of the late N and O intermediates and time constants T_4 and T_5 correspond to their decay and the return to the pR ground state. The time constants are listed in Tables 3 and 4.

The *E. coli* membrane consists mostly of PE (~75%) and PG (~25%) (see Section 3.2). In addition to these lipids, we have included PC in our study of head group effects, because it is also a zwitter-ionic lipid like PE that is often used in functional studies as a replacement for PE. While PE is cone shaped, PC due to its larger head group has a more cylindrical shape and thus much better bilayer forming properties than PE. In contrast to PE and PC, the second most abundant lipid in *E. coli* PG is negatively charged.

Fig. 4 shows the effect of the lipid head group on the photocycle. In these experiments, we aimed to use di-oleyl as lipid acyl chains with all head groups, but we failed to form bicelles with 1,2-dioleoyl-*sn*-glycero-3-phosphoethanolamine (DOPE) since the lipid film did not dissolve in the CHAPS containing buffer. Instead we obtained bicelles with 1-palmitoyl-2-oleoyl-*sn*-glycero-3-phosphoethanolamine (POPE). The difference between POPC and DOPC regarding one of the acyl chains did not alter the photocycle as shown in Fig. 6 and by the time constants in Table 3. Therefore, it is assumed that POPE is a valid replacement for DOPE in this experiment.

The results for the two lipids with zwitter-ionic head groups, DOPC and POPE, are shown in panel A of Fig. 4. Very similar kinetics at all wavelengths were observed (see Table 3). The signal of the late intermediates (at 580 and 630 nm) was larger for POPE. One of the reasons is a somewhat faster formation of the late intermediates with POPE (2.2 ms for POPE and 3.0 ms for DOPC, see Table 3) which can result in a higher population of these intermediate states. Another reason could be a stronger absorption of the late intermediates in the POPE environment. We ascribe the observed effect to the different head groups of the two lipids, since the acyl chain difference has very little effect on the photocycle (compare DOPC and POPC in Table 3 and Fig. 6A).

When the negatively charged DOPG was used (pink trace in Fig. 4B), the decay of the signal at 410 nm was accelerated. This clear effect is only to a minor degree due to a change in the reaction kinetics, since the two time constants T_2 and T_3, which describe the two phases of the decay, are only affected to a small extent (Table 3). Instead, the effect is caused by a much larger contribution of the fast phase in the case of DOPG (80%) than in the cases of DOPC and POPE (40%). The two phases possibly reflect the decay of the M_1 and M_2 intermediates

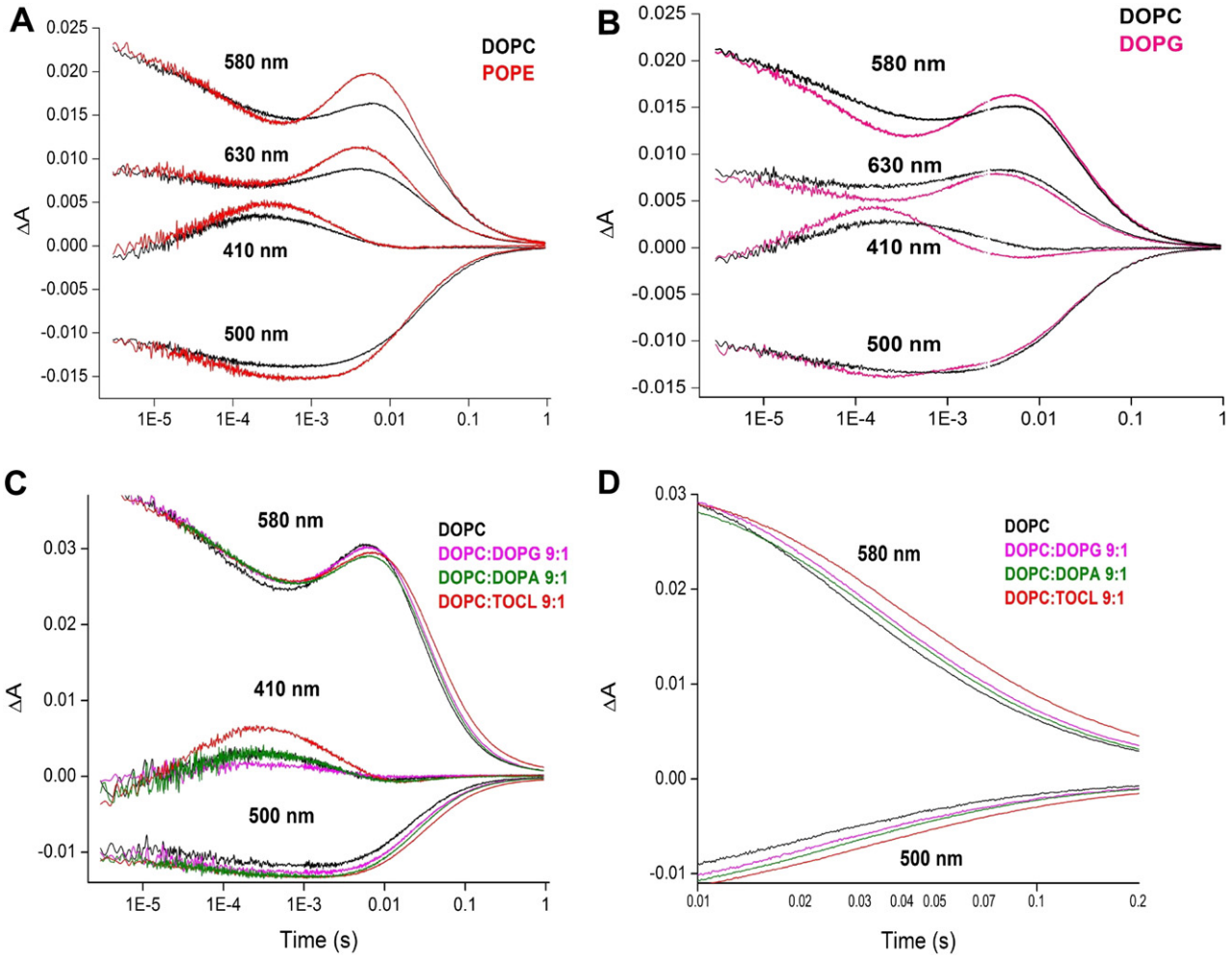

Fig. 4. Modulation of the pR photocycle by lipids of different charges. DOPG, DOPA and TOCL are anionic, whereas POPE and DOPC are zwitter-ionic. The transient absorption changes were induced by a laser pulse (532 nm, 10 ns pulse). The traces represent the averages of 10 single turnover experiments. Comparison of bicelles containing (A) DOPC and POPE, (B) DOPC or DOPG, and (C) DOPC with or without admixture of 10% of different anionic lipids. (D) Traces of (C) shown on an expanded scale.

[8] and the different contributions of the two phases in different lipid systems might indicate a different equilibrium constant between M_1 and M_2.

In the next measurements, we investigated further the influence of negatively charged lipids on the photocycle of pR. These experiments were performed with a new pR preparation (preparation 2). The bicelles contained DOPC as lipid matrix and different anionic lipids in a 9/1 ratio. At the pH of our measurements (pH 7.8), the charge of DOPG is −1, that of 1,2-dioleoyl-*sn*-glycero-3 phosphate (DOPA) approximately −1.5, and that of tetraoleoyl cardiolipin (TOCL) −2. The time constants and rates for these systems are listed in Table 4. The experimental data are shown in Fig. 4C and on an expanded scale also in Fig. 4D. They reveal small but systematic effects upon the addition of negatively charged lipids. This is most clearly seen in Fig. 4D: the return to the ground state absorbance at 500 and 580 nm is slower when the negative charge of the minor lipid increases. The effect can be explained by the slightly different time constants for T_4 and T_5 obtained in the fit (Table 4). However, most of them are equal within the error limits, indicating that the reaction kinetics are essentially unchanged.

3.8. Effect of membrane thickness on the pR photocycle

To test the influence of membrane thickness on the photocycle, pR was reconstituted in bicelles with lipids having a PC head group and different fatty acid chain lengths. Fig. 5 shows the effects of different lipid chain lengths, ranging from 14 to 20 C-atoms, on the photocycle. In addition to these acyl chain lengths, a sample with 22:1 PC was also prepared but was not translucent and exhibited strong light scattering, which indicated aggregation, probably due to hydrophobic mismatch between pR and the detergent/lipid environment. Therefore, we did not further investigate this sample.

In all other cases, the kinetics of formation of the M-intermediate were hardly affected by the chain length (τ ~40 μs, Table 3) and the intermediate decayed within the same time frame (T_2 and T_3 in Table 3). In spite of the similar kinetics of M intermediate formation and decay, the amplitude of the signal at 410 nm is considerably larger for the shortest chain length (Fig. 5A). This could be due to an overall stronger absorption of the M intermediate in this lipid environment. Either all M substates are similarly affected or different M intermediates have different absorption coefficients and the stronger absorbing intermediate is more populated when the lipid chains are shorter.

Another amplitude effect is observed for the 580 and 630 nm signals which are smaller for the two shorter lipids in the sub-millisecond range. This is likely due to a reduced absorption of the K intermediate.

While being similar, the decay of the late intermediates (Fig. 5C and D) and restoration of the ground state (Fig. 5B) are influenced by the fatty acid chain length, showing a slower turnover for the protein in lipids with the shortest chain lengths (see Fig. 5B–D). This is also

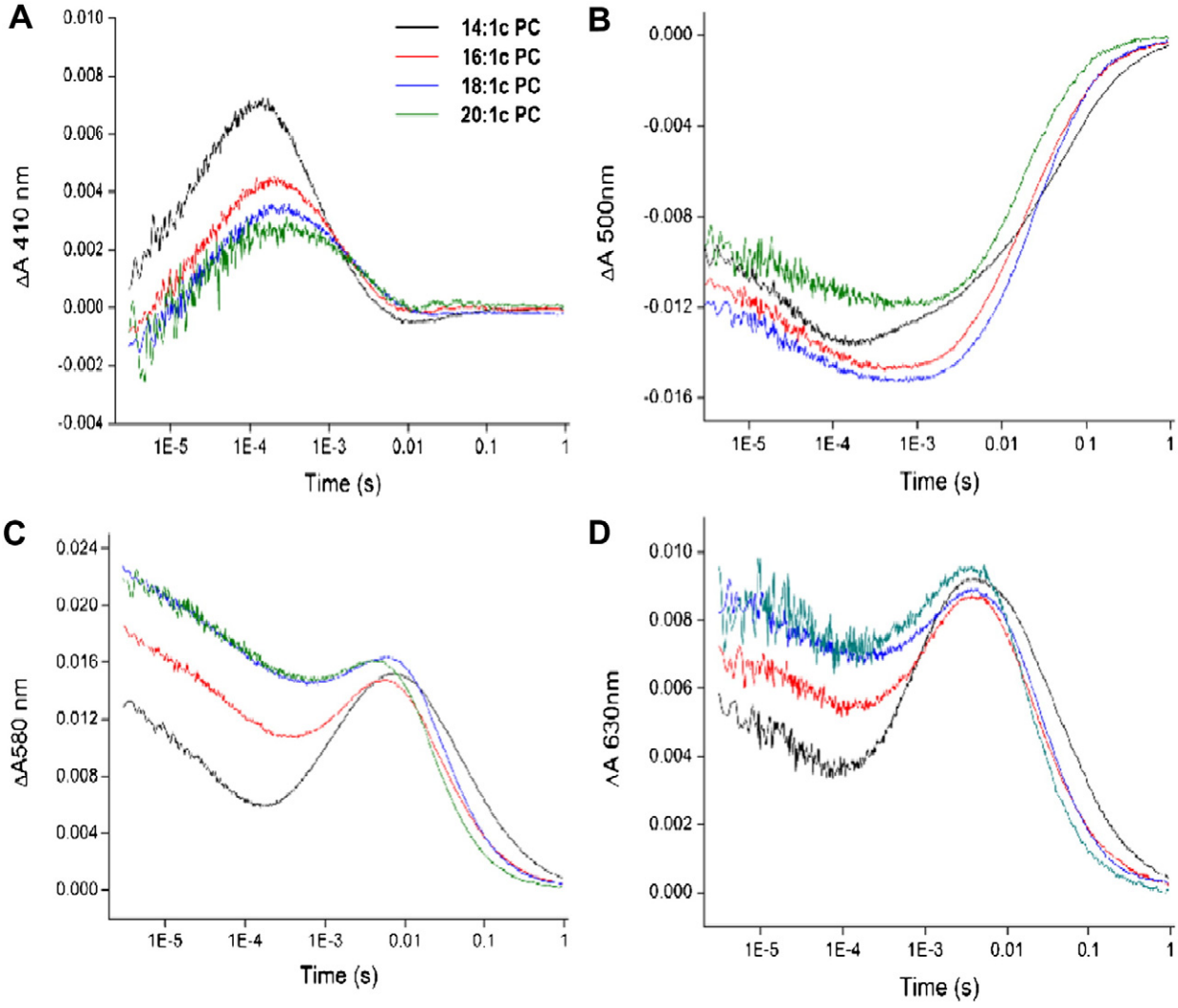

Fig. 5. The effect of acyl chain length on the pR photocycle. Photocycle kinetics were recorded at 410 nm (A), 500 nm (B), 580 nm (C) and 630 nm (D) for pR preparations in PC bicelles with 14:1 PC (DMoPC), 16:1 PC, 18:1 PC (DOPC), and 20:1 PC acyl chains.

reflected in the time constants T_4 and T_5 (Table 3) which describe the return to the ground state. They are 31 and 167 ms in the presence of the 14:1 lipid, but near 20 and 100 ms with longer acyl chains. The photocycle is apparently slower with the 16 and 18 C chains than with the 20 C chains (see Fig. 5B–D), but this is not revealed in the time constants. Therefore, the effect must be due to a larger proportion of the faster phase (described by T_4) than of the slowest phase (described by T_5) in the 20 C system. Possible reasons for the different contributions of the two phases are different absorption spectra of the intermediates and different equilibrium constants between the intermediates in the different lipid systems.

3.9. Effects of saturation vs unsaturation of fatty acid chains

For the lipids tested above we chose predominantly fatty-acyl chains with one *cis* double bond (18:1) which are abundant in *E. coli* membranes. Fatty acids of 18:0 type are less abundant, while the situation is inverse for lipids with chain lengths of 14 and 16 carbons (i.e. 14:0 and 16:0 lipids are more abundant than 14:1 and 16:1 lipids). Here, the effect of a double bond on the photocycle was tested for 14 C and 16 C-18 C chain lengths by using bicelles composed of the phospholipids 1,2-dimyristoleoyl-*sn*-glycero-3-phosphocholine (14:0, DMPC) and 14:1 (Δ9-cis) PC (1,2-dimyristoyl-*sn*-glycero-3-phosphocholine, DMoPC) as well as DOPC (18:1, Δ9-cis) and POPC (16:0–18:1, Δ9-cis). The phase transition temperature of pure DMPC is close to room temperature. Nevertheless, temperature dependent ^{31}P NMR spectra of our CHAPS/DMPC bicelles confirmed that the lipids are in the fluid phase, presumably due to the presence of the detergent.

Fig. 6A compares the photocycle with DOPC and POPC. The switch from DOPC to POPC involves removal of the double bond in one of the chains as well as a reduction of the length of this chain by 2 carbon atoms. The length change is not expected to have a significant effect on the photocycle. This is evident from the above discussion of Fig. 5, which revealed that the kinetics of the photocycle are very similar for lipids with chain lengths of 16 and 18 C atoms and with one double bond in both acyl chains. When one of the unsaturated 18 C acyl chains is replaced by a 16 C saturated chain, the traces were again similar at all wavelengths (Fig. 6A) and the time constants are identical within the error limits (Table 3). This indicates little influence of unsaturation on the kinetics when the acyl chains have 16–18 carbon atoms.

More pronounced effects of unsaturation were observed for 14 C chains (Fig. 6B), in particular regarding the formation of the late intermediates (described by T_3), which is faster with DMoPC. Common for the two short chain lipids DMPC and DMoPC is that the return to the ground state is slower than for lipids with longer chains.

The DMoPC environment provides the most distinct differentiation between the late intermediates since the maximum of the 630 nm trace is reached earlier than the maximum of the 580 nm trace. This is true also for other lipid systems, but the effect is most clearly observed for DMoPC. The different time points for the maxima are in line with the proposed photocycle [7,8] where the O intermediate, which has the most red shifted absorption maximum, is formed before the N intermediate, which absorbs at shorter wavelengths and similar to pR.

4. Discussion

4.1. Identification of lipids that bind to pR

Even though the native lipid environment for all organisms overexpressing pR is not known, a prediction of abundant lipids was obtained through an analysis of the genomes of host organisms for the presence of enzymes which synthesize relevant lipids. From this analysis, the native lipid environment for pR seems to be similar to the *E. coli* lipid composition, in which the protein was overexpressed for this study. The *E. coli* membrane comprises 70–80% PE, 20–25% PG and ~5% cardiolipin with a variety of acyl chain lengths ranging between 14 and 19 carbons. Consequently, the majority of the head groups are of zwitter-ionic nature and have a non-bilayer character.

Many membrane proteins bind specific lipids [47]. For pR, we found that 10 PE molecules were co-purified per pR molecule at a DDM concentration of 0.1%. Less than 1 PG molecule per pR molecule was retained under these conditions. Both of these lipids migrated further from their respective bulk lipids on the TLC plates, which indicates that pR selects a lipid subpopulation which is less polar. We conclude that the innermost shell of lipids around pR is predominantly composed of less polar species of the main *E. coli* lipid PE.

4.2. The bicelle model system

We investigated the effects of the lipid environment on the photocycle of pR in flash photolysis experiments using bicelles consisting of CHAPS and synthetic lipids. The CHAPS/lipid isotropic bicelles have been characterized earlier [44]. The study showed that the phospholipids and the detergents within the bicelles are separated in a bilayer region and a detergent rim. We used bicelles with a q = [lipid]/[CHAPS] = 0.5, which are known to be smaller than DMPC/DHPC bicelles, but likewise stable over time [44]. Bicelles are a good system to test membrane parameters regarding their effects on the function of membrane proteins in a systematic way. The system allows testing lipids like POPE while it would be difficult to make liposomes from the pure POPE lipid. Reconstitution of pR in bicelles was a

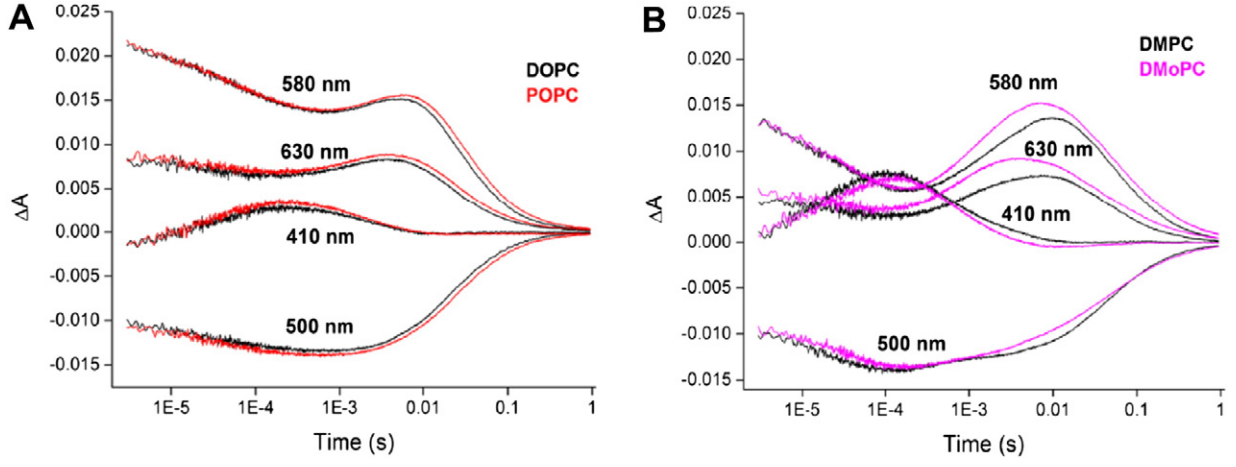

Fig. 6. Effects of unsaturation of the acyl chains on the pR photocycle. (A) 18:1 PC (DOPC) and 16:0–18:1 PC (POPC). (B) 14:0 PC (DMPC) and 14:1 PC (DMoPC).

convenient route to test a variety of lipids, keeping the light scattering in the sample to a minimum, which is beneficial for spectroscopic experiments.

4.3. Photocycle summary

The effects of lipids on the photocycle were followed spectroscopically at 410 nm (monitoring formation and decay of the M state), at 500 nm (photoisomerization, formation and decay of N, and reformation of the ground state) and at 580 and 630 nm, where mainly the K and O intermediates of the cycle are observed. Complete photocycles were obtained for all pR preparations. The photocycle was fastest in liposomes, intermediate in bicelles and Triton X-100 and slowest in CHAPS. These data indicate that pR activity is indeed dependent on the lipid environment. CHAPS, known as a stiff detergent, is expected to restrict the protein motion and the drastically slowed down photocycle indicated that motional flexibility is required for maximal pR activity. Noteworthy, bicelles containing a mixture of CHAPS and lipids restored much of the activity. This indicates that pR is now in a lipidic environment and is in accordance with the notion of spatial separation between lipids and detergent in bicelles mentioned above. However, no bicelle sample had a similar turnover speed as pR reconstituted in liposomes. This can indicate that residual CHAPS molecules are still bound to pR, that the packing of the bilayer is different in bicelles and in liposomes, or that the oligomeric state of pR is different.

Different lipids in the bicelles affect the photocycle to some extent and lead to a variation of all five time constants by a factor of 2. This corresponds to a rather small variation in activation energies of the respective partial reactions, which amounts to less than 2 kJ/mol. This energy difference is much less than the energy of a typical hydrogen bond (10–20 kJ/mol), indicating that the kinetic effects are brought about by minor structural adjustments. The limited variation in the time constants demonstrates that pR is a robust protein which works in many different lipid environments. Apart from the time constants, the absorbance spectra of the intermediates or the equilibria between them are affected by the lipid environment. This indicates that the membrane environment can modify the structure of pR and that some of these changes influence the electronic states of the retinal.

4.4. Effects of lipid head groups on the photocycle of pR

Different lipid head groups have little effect on the kinetics of the photocycle as demonstrated by the similar time constants in Tables 3 and 4. The negatively charged DOPG seems to modify the weight of the slow and the fast phase of M decay (pink trace in Fig. 4B), possibly because of a shifted equilibrium between the two M states M_1 and M_2.

4.5. Effects of bilayer thickness on the photocycle of pR

Another characteristic of the cell membrane is the thickness of the bilayer, which is determined by the length of the fatty acid chains of the phospholipids. The experiments on bicelles with different bilayer thicknesses revealed that functional pR requires bilayers with a hydrophobic thickness of 20 carbons or less. When pR was reconstituted in a fixed pR/bicelle ratio, a higher incorporation of pR in shorter chain length lipids was observed with the highest incorporation found for 14 C lipids (data not shown). Lipids with chains shorter than 14 carbons were not tested as they are not common in the membranes of the organisms where pR naturally occurs. Chains longer than 14 C atoms accelerate the decay of the late intermediates and the overall turnover. Additionally, the absorbance spectrum of the early K and M intermediates is affected. These results indicate that pR adapts its conformation to fit the bilayer thickness without dramatically changing its reaction kinetics.

4.6. Effects of lipid unsaturation on the photocycle of pR

Unsaturation was found to have little effect on the photocycle when the acyl chains are long (18 carbons). For shorter chains a particularly interesting effect of unsaturation is that the O intermediate is formed significantly earlier than the N intermediate. This good separation of the time window of accumulation of these two intermediates implies that a convenient system to study the O to N transition would be bicelles containing unsaturated lipids with short chains.

4.7. Comparison to previous work

While our work is the first systematic approach to test the lipid influence on pR using a bicelle system, information on lipid effects on the pR photocycle has been obtained by other groups [25], where they reconstituted pR into nanodiscs and found an about two-times slower photocycle in DMPC than in DOPC, matching our findings (Table 3). Direct comparison of the rates is not possible because of different mathematical models. Recently, Mörs et al. [48] have compared the photocycle of pR in liposomes and nanodiscs composed of DMPC/DMPA = 9/1 and found time constants that are very similar to ours. The time constants of our DMPC bicelle preparation are very similar to both preparations for the fast reactions and only ~1.5 times slower for the two slowest phases, reinforcing the validity of our system as lipid mimetic.

5. Conclusions

Predominantly lipids with PE head group that are less polar than the corresponding bulk lipids were found to associate with pR. They do not bind with high affinity since they can be removed by increased detergent concentration. Therefore, the retained PE at low detergent concentration most likely represents the inner shell of lipids around pR in *E. coli* membranes. In spite of pR's preference for certain types of lipid, it does not seem to require particular lipids for function. This finding is different from results obtained for bR, which requires certain types of lipids for optimum activity [24]. In the case of pR, lipid properties have instead only a mild influence on its function. They modulate the kinetics of the photocycle and the absorption of the intermediates to some extent, with chain length having the most pronounced effect. We conclude that pR thrives in many different lipid systems, in particular in the *E. coli* membrane environment, which consists predominantly of the zwitter-ionic phospholipid PE with chain lengths of 16 to 18 carbons. In our experiments, these conditions sustain the fastest turnover rates.

The photocycle turnover was fastest in liposomes, intermediate in all investigated bicelles and in the detergent Triton X-100 and slowest in the detergent CHAPS. This difference between bicelles and liposomes might be due to remaining bound CHAPS molecules, due to a different oligomeric organization of pR, or point towards the importance of collective bilayer properties. Nevertheless, the bicelle is a convenient system to study the function of pR, since it is closer to the native bilayer membrane environment than detergent solubilized pR, since the photocycle involves all intermediates, and because of the reduced light scattering as compared to liposomes.

Dedication

We would like to dedicate this work to Professor Åke Wieslander, who sadly passed away before the submission of this manuscript. His enthusiasm and knowledge were a source of inspiration for all coauthors.

Transparency document

The Transparency document associated with this article can be found in the online version.

Acknowledgements

Carl Tryggers Foundation provided a post-doctoral stipend to Ljubica Lindholm and the Swedish Research Council (2006-4818) supported Candan Ariöz. Christoph von Ballmoos was holder of a fellowship for young researchers from the Swedish Research Council. We thank Nikolaos Daskalakis for help with the light driven proton pumping assay.

References

[1] O. Béjà, L. Aravind, E.V. Koonin, M.T. Suzuki, A. Hadd, L.P. Nguyen, S.B. Jovanovic, C.M. Gates, R.A. Feldman, J.L. Spudich, E.N. Spudich, E.F. DeLong, Bacterial rhodopsin: evidence for a new type of phototrophy in the sea, Science 289 (2000) 1902–1906.
[2] J.R. de la Torre, L.M. Christianson, O. Beja, M.T. Suzuki, D.M. Karl, L. Heidelberg, E.F. DeLong, Proteorhodopsin genes are distributed among divergent marine bacterial taxa, Proc. Natl. Acad. Sci. 100 (2003) 12830–12835.
[3] N.U. Frigard, A. Martinez, T.J. Mincer, E.F. DeLong, Proteorhodopsin lateral gene transfer between marine planktonic Bacteria and Archaea, Nature 439 (2006) 847–850.
[4] J.M. Gonzalez, B. Fernandez-Gomez, A. Fernandez-Guerra, L. Gomez-Consarnau, O. Sanchez, M. Coll-Llado, J. Del Campo, L. Escuadero, R. Rodrigez-Martinez, L. Alonso-Saez, M. Latasa, I. Paulsen, O. Nedeshkovskaya, I. Lukenberri, J. Pinhassi, C. Pedro-Alio, Genome analysis of the proteorhodopsin-containing marine bacterium *Polaribacter* sp. MED152 (Flavobacteria), Proc. Natl. Acad. Sci. 105 (2008) 8724–8729.
[5] C. Sanchez, Horizontal gene transfer: eukaryotes under a new light, Nat. Rev. Microbiol. 9 (2011) 228–229.
[6] N. Yutin, E.V. Konin, Proteorhodopsin genes in giant viruses, Biol. Direct 7 (2012) 34–37.
[7] T. Friedrich, S. Geibel, R. Kalmbach, I. Chizhov, K. Ataka, J. Heberle, M. Engelhard, E. Bamberg, Proteorhodopsin is a light-driven proton pump with variable vectoriality, J. Mol. Biol. 321 (2002) 821–838.
[8] G. Varo, L.S. Brown, M. Lakatos, J.K. Lanyi, Characterisation of the photochemical reaction cycle of proteorhodopsin, Biophys. J. 84 (2003) 1202–1207.
[9] C.L. Dupont, D.B. Rusch, S. Yooseph, M. Lombardo, R.A. Richter, R. Valas, M. Novotny, J. Yee-Greenbaum, J.D. Selengut, D.H. Haft, A.L. Halpern, R.S. Lasken, K. Nealson, R. Friedman, J.C. Venter, Genomic insights to SAR86, an abundant and uncultivated marine bacterial lineage, ISME J. 6 (2012) 1186–1199.
[10] E.P. Ivanova, N.V. Zhukova, V.I. Svetashev, N.M. Gorshkova, V.V. Kurilenko, G.M. Frolova, V.V. Mikhailov, Evaluation of phospholipid and fatty acid compositions as chemotaxonomic markers of *Alteromonas*-like proteobacteria, Curr. Microbiol. 41 (2000) 341–345.
[11] J.M. Gonzalez, J. Pinhassi, B. Fernandez-Gomez, M. Coll-Llado, M. Gonzalez-Velazquez, P. Pigbo, S. Jaenicke, L. Gomez-Consarnau, A. Fernandez-Guerra, A. Goesmann, C. Pedroz-Alio, Genomics of the proteorhodopsin-containing marine flavobacterium *Dokdonia* sp. strain MED134, App. Environ. Microbiol. 77 (2011) 8676–8686.
[12] Y. Jiang, D.Y. Sorokin, R. Kleerebezem, G. Muyzer, M. van Loosdrecht, *Plasticicumulans acidovorans* gen. nov., sp. nov., a polyhydroxyalkonoate-accumulating gammaproteobacterium from a sequencing-batch bioreactor, Int. J. Syst. Evol. Microbiol. 61 (2011) 2314–2319.
[13] M. Fahrbach, J. Kuever, M. Remesh, B.E. Huber, P. Kampfer, W. Dott, J. Hollender, *Steroidobacter denitrificans* gen. nov., sp. nov., a steroidal hormone-degrading gammaproteobacterium, Int. J. Syst. Evol. Microbiol. 58 (2008) 2215–2223.
[14] N. Tanaka, L.A. Romanenko, T. Iino, G.M. Frolova, V.V. Mikhailov, *Cocleimonas flava* gen. nov., sp. nov., a gammaproteobacterium isolated from sand snail (*Umbonium costatum*), Int. J. Syst. Evol. Microbiol. 61 (2011) 412–416.
[15] W. Dowhan, Molecular basis for membrane phospholipid diversity: why are there so many lipids, Annu. Rev. Biochem. 66 (1997) 199–232.
[16] Y. Kanemasa, Y. Akamatsu, S. Nojima, Composition and turnover of the phospholipids in *Escherichia coli*, Biochim. Biophys. Acta 144 (1967) 382–390.
[17] A.N. Bondar, C. del Val, S.H. White, White Rhomboid protease dynamics and lipid interactions, Structure 17 (2009) 395–405.
[18] O.S. Andersen, R.E. Koeppe, Bilayer thickness and membrane protein function: an energetic perspective, Annu. Rev. Biophys. Biomol. Struct. 36 (2007) 107–130.
[19] M.Ø. Jensen, O.G. Mouritsen, Lipids do influence protein function— the hydrophobic matching hypothesis revisited, Biochim. Biophys. Acta 1666 (2004) 205–226.
[20] A.P. Starling, K.A. Dalton, J.M. East, S. Oliver, A.G. Lee, Effects of phosphatidylethanolamines on the activity of the Ca^{2+}-ATPase of sarcoplasmic reticulum, Biochem. J. 320 (1996) 309–314.
[21] K. Pfeiffer, V. Gohil, R.A. Stuart, C. Hunte, U. Brandt, M.L. Greenberg, H. Schagger, Cardiolipin stabilizes respiratory chain supercomplexes, J. Biol. Chem. 278 (2003) 52873–52880.
[22] F.I. Valiyaveetil, Y. Zhou, R. MacKinnon, Lipids in the structure, folding, and function of the KcsA K^+ channel, Biochemistry 41 (2002) 10771–10777.
[23] M.K. Joshi, S. Dracheva, A.K. Mukhopadhyay, S. Bose, R.W. Hendler, Importance of specific native lipids in controlling the photocycle of bacteriorhodopsin, Biochemistry 37 (1998) 14463–14470.
[24] A.K. Mukhopadhyay, S. Dracheva, S. Bose, R.W. Hendler, Control of the integral membrane proton pump, bacteriorhodopsin, by purple membrane lipids of *Halobacterium*, Biochemistry 35 (1996) 9245–9252.
[25] M.J. Ranaghan, C.T. Schawall, N.N. Alder, R.R. Birge, Green proteorhodopsin reconstituted into nanoscale phospholipid bilayers (nanodiscs) as photoactive monomers, J. Am. Chem. Soc. 45 (2011) 18318–18327.
[26] B. Miroux, J.E. Walker, Over-production of proteins in *Escherichia coli*: mutant host that allows synthesis, J. Mol. Biol. 260 (1996) 289–298.
[27] N. Pfleger, M. Lorch, A.C. Woerner, S. Shastri, C. Glaubitz, Characterisation of Schiff base and chromophore in green proteorhodopsin by solid-state NMR, J. Biomol. NMR 40 (2008) 15–21.
[28] E.G. Bligh, W.J. Dyer, A rapid method of total lipid extraction and purification, Can. J. Biochem. Physiol. 37 (1959) 911–917.
[29] G. Sezanov, D. Joseleau-Petit, R. D'Ari, *Escherichia coli* physiology in Luria–Bertani broth, J. Bacteriol. 189 (2007) 8746–8749.
[30] J. Cladera, J. Rigaud, J. Villaverde, M. Dunach, Liposome solubilization and membrane protein reconstitution using CHAPS and CHAPSO, Eur. J. Biochem. 243 (1997) 798–804.
[31] M. Branden, A. Hamslauer, R.B. Gennis, P. Adelroth, P. Brzezinski, On the role of the K-proton transfer pathway in cytochrome c oxidase, Proc. Natl. Acad. Sci. 98 (2001) 5013–5018.
[32] K.A. Johnson, Z.B. Simpson, T. Blom, Global kinetic explorer: a new computer program for dynamic simulation and fitting of kinetic data, Anal. Biochem. 387 (2009) 20–29.
[33] K.A. Johnson, Z.B. Simpson, T. Blom, FitSpace explorer: an algorithm to evaluate multidimensional parameter space in fitting kinetic data, Anal. Biochem. 387 (2009) 30–41.
[34] E.O. Stejskal, J.E. Tanner, Spin diffusion measurements: spin echoes in the presence of a time-dependent field gradient, J. Chem. Phys. 42 (1965) 288–292.
[35] P.T. Callaghan, M.E. Komlosh, M. Nyden, High magnetic field gradient PGSE NMR in the presence of a large polarizing field, J. Magn. Reson. 133 (1998) 177–182.
[36] E.V. Meerwall, M. Kamat, Effect of residual field gradients on pulsed-gradient NMR diffusion measurements, J. Magn. Reson. 83 (1989) 309–323.
[37] K. Nomura, M. Lintuluoto, K. Morigaki, Hydration and temperature dependence of ^{13}C and ^{1}H NMR spectra of the DMPC phospholipid membrane and complete resonance assignment of its crystalline state, J. Phys. Chem. B 115 (2011) 14991–15001.
[38] L. Longsworth, The mutual diffusion of light and heavy water, J. Phys. Chem. 64 (1960) 1914–1917.
[39] C.R. Cantor, P.R. Schimmel, Biophysical Chemistry: Part II: Techniques for the Study of Biological Structure and Function 2, Macmillan, 1980.
[40] H. Biverståhl, J. Lind, A. Bodor, L. Mäler, Biophysical studies of the membrane location of the voltage-gated sensors in the HsapBK and KvAP K^+ channels, Biochim. Biophys. Acta 1788 (2009) 1976–1986.
[41] C. Yang, M. Chen, A.B. Arun, C.A. Chen, J. Wang, W. Chen, *Endozoicomonas montiporae* sp. nov., isolated from the encrusting pore coral *Montipora aequituberculata*, Int. J. Syst. Evol. Microbiol. 60 (2010) 1158–1162.
[42] W. Dowhan, Molecular genetic approaches to defining lipid function, J. Lipid Res. 50 (2009) S305–S310.
[43] C. Ariöz, H. Götzcke, L. Lindholm, J. Eriksson, K. Edwards, D.O. Daley, A. Barth, A. Wieslander, Heterologous overexpression of a monotopic glycosyltransferase (MGS) induces fatty acid remodeling in *Escherichia coli* membranes, Biochim. Biophys. Acta 1838 (2014) 1862–1870.
[44] A. Andersson, L. Mäler, Magnetic resonance investigations of lipid motion in isotropic bicelles, Langmuir 21 (2005) 7702–7709.
[45] J. Lipfert, L. Columbus, V.B. Chu, S.A. Lesley, S. Doniach, Size and shape of detergent micelles determined by small-angle X-ray scattering, J. Phys. Chem. B 111 (2007) 12427–12438.
[46] X. Quin, M. Liu, D. Yang, X. Zhang, Concentration-dependent aggregation of CHAPS investigated by NMR spectroscopy, J. Phys. Chem. B 114 (2010) 3863–3868.
[47] C. Hunte, Specific protein–lipid interactions in membrane proteins, Biochem. Soc. Trans. 33 (2005) 938–942.
[48] K. Mörs, C. Roos, F. Scholz, J. Wachveitl, V. Dötsch, F. Bernhard, C. Glaubitz, Modified lipid and protein dynamics in nanodiscs, Biochim. Biophys. Acta 1828 (2013) 1222–1229.